The $\phi - \Theta$ interference from g12 experiment. Preliminary results.

M. Amaryan, G. Gavalian, C. Nepali, M. Polyakov and L. Weinstein

1 Introduction

One of the main scientific principles to establish unknown phenomena is it's reproducibility in a different independent experiments. Although one would prefer to not change conditions of the experiment being conducted, nevertheless manifestation of the signal in the new measurement has decisive impact on the acceptance of results and the final conclusion.

As it is already well known within the CLAS Collaboration, the g11 data analysis by ODU group has led to the observation of narrow resonance structure in the missing mass of K_S in the photoproduction reaction $\gamma + p \rightarrow K_s(\pi^+\pi^-)pX$ for events selected under the ϕ meson peak, which is reconstructed in the missing mass of the recoil proton in the same reaction. Multiple notes and extensive supporting information on the above mentioned analysis can be found in the CLAS Hadron Spectroscopy Working Group secure web page.

The g12 experiment run on hydrogen target and is considered to be potentially testing experiment for results obtained from g11 experiment.

Before going into details and concrete results let us mention similarities and differences of data from g11 and g12 experiments.

1. Both experiments run using tagged photon beam and hydrogen target with the CLAS setup.

2. However g11 experiment used electrons with the beam energy of E_e=3.5 GeV to produce bremsstrahlung photons, while g12 experiment used electrons with the beam energy of $E_e = 5.75$ GeV.

3. The g11 experiment collected two opposiltely charged tracks with open trigger in the full range of photon energies. The g12 experiment was approved primarily to run at photon energies above

$E_\gamma > 4$ GeV, however additional trigger was set up for three charged tracks for lower photon energies.

4. The liquid hydrogen target in the g12 experiment was moved 90 cm upstream compared to it's position during the g11 run.

5. An overall acceptance of two experiments is significantly different.

It is clear that the g12 experiment is not an exact repetition of the g11 experiment, nevertheless the resonance structure observed in in the g11 experiment is expected to manifest also in the g12 data, if it is not a fake signal or some sort of statistical fluctuation accompanying searches of the Θ^+ pentaquark.

2   The g12 Data Analysis

In this section we present results from the g12 experiment PASS1 cooked data. Note that all techniques developed for the event reconstruction in the g11 data analysis is applied *blindly* to reconstruct events in the g12 data.

The primary vertex, the decay vertex and the collinearity angle are defined in exactly the same way as in the g11 analysis.

Below fig. 1 we present a few main distributions from subsample of g12 data to see how well we reconstruct all known particles that are relevant for this analysis. These are : a) the invariant mass of two pions with all vertex cuts (see below); b) the missing mass of K_s to reconstruct well known $\Sigma^+(1190)$ and $\Sigma^{*+}(1385)$ resonances; c) the missing mass of pK_s system to reconstruct another missing kaon; d) the missing mass of the proton, to reconstruct the ϕ meson.

To obtain these figures the following cuts have been applied:

- The proton track is selected to be within the circle of 2 cm diameter around the photon beamline.

- The distance of the closest approach of two pion tracks to be less than 1 cm.

- The collinearity angle, the angle between the line connecting mid points of two pion tracks and the mid point of the proton-photon closest distance on one side and the three-momentum vector of two pions on ther side to be $\cos\theta > 0.98$.

- When necessary, the $\pm 2\sigma$ cuts are applied around masses of the particles.

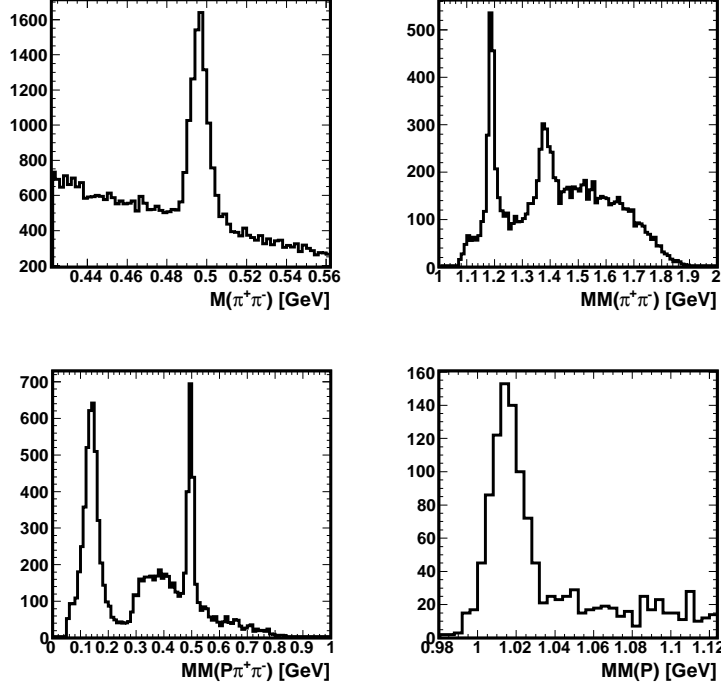- To be consistent with g11 analysis the photon energy range is limited to E_γ=(1.6-2.6) GeV.

Figure 1: Experimental distributions from g12 Data: a) invariant mass of two pions; b) missing mass of two pions; c) missing mass of $P\pi^+\pi^-$ system wihin $M(\pi^+\pi^-) = 0.495\pm0.01$ GeV; d) missing mass of the proton with the cuts on $M(\pi^+\pi^-) = 0.495\pm0.01$ GeV and $\mathbf{MM}(P\pi^+\pi^-) = 0.497\pm 0.02$ GeV.

Although g12 Data are still being polished and momentum corrections have not been yet applied, still as one can see all distributions reproduce expected particles quite well. At this stage we do not address whether exact positions of K_S, K_L, Σ hyperons and ϕ meson coincide with their PDG values.

On the next fig. 2 we present photon energy distribution for entire data set of g12 data together with the same distibution from g11 data for events selected under the ϕ peak with all cuts described above to obtain fig. 1d).
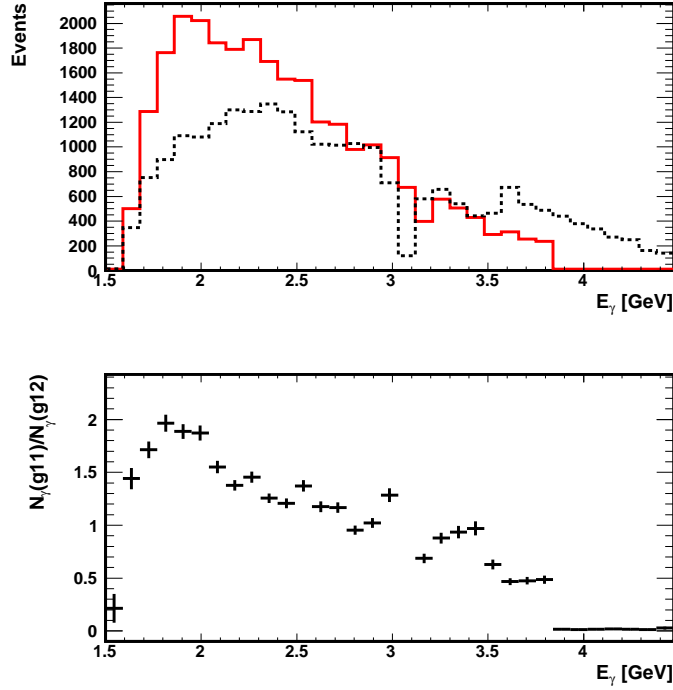

Figure 2: Upper panel: photon energy distribution for events selected under the ϕ peak reconstructed with the same cuts from g11 data (solid histogram) and g12 (dashed histogram). Lower panel: ratio of number of photons from g11 and g12 data versus photon energy.

As one can see due to the trigger suppression in g12 data, the pho-

ton energy range below 2.1 GeV in the region of the overlap of the ϕ meson and possible baryon resonance with the mass around $M(pK^0) \approx$ 1.54 GeV is significantly suppressed. It means that first of all statistical power of g12 data is less than one would naively expect due to the better running conditions of higher beam current and secondly the whole spectrum of the photons is deformed giving preference for the production of higher baryon masses.

In fig. 3 missing mass of K_s is presented for g11 data with a cut on $-t_\Theta < 0.45$ GeV and for g12 data with different t cuts with photon energy range for all histograms in the range $E_\gamma = 1.6 - 2.6$ GeV. As it is expected the shape of the distribution in g12 data is very different from that of g11 data as the range of photon energies below $E_\gamma < 2.1$ GeV is significantly suppressed in g12 data.

In fig. 4 missing mass of K_s is plotted versus photon energy for events selected under the ϕ peak. As one can see effective region contributing to the $\mathrm{MM}(K_S) \approx 1.54$ GeV is within the range $E_\gamma = 1.75 - 2.1$ GeV.

It is even more compelling if one looks at plots where $\mathrm{MM}(K_S)$ is plotted versus MM(p) for different ranges of photon energy. In fig. 5 left panel is for $E_\gamma < 1.75$ GeV, middle panel is for $E_\gamma = 1.75 - 2.0$ GeV and the right panel is for $E_\gamma > 2.1$ GeV. It is clear that left panel and the right panel do not access region of $\mathrm{MM}(K_S) \approx 1.54$ GeV, while the region of the photon energies $E_\gamma = 1.75 - 2.1$ GeV covers $\mathrm{MM}(K_S)$ from the threshold up to 1.65 GeV.

In fig. 6 we present missing mass of kshort with no cuts on t_Θ and with open photon energy cut $E_\gamma = 1.6 - 2.6$ GeV (upper panel), with energy range $E_\gamma = 1.75 - 2.1$ GeV (red histogram) and otside of this energy range combined (blue) histogram. As one can see by ignoring the energy range of the overlap of ϕ and baryon resonance around 1.54 GeV it is possible to deform missing mass distribution to the degree when baryon resonance will be buried in the background from irrelevant neighboring energy ranges. These one dimensional projections of fig. **??** underline the necessity to select the range of $E_\gamma = 1.75 - 2.1$ GeV even more explicitly.

Similar distributions for $t_\Theta < 0.45$ GeV^2 from g11 data are presented in fig. 7 together with ϕ-MC simulated data with normalization done outside of the photon energy range where the baryon resonance structure is observed at ≈ 1.54 GeV. The data and MC histograms on the
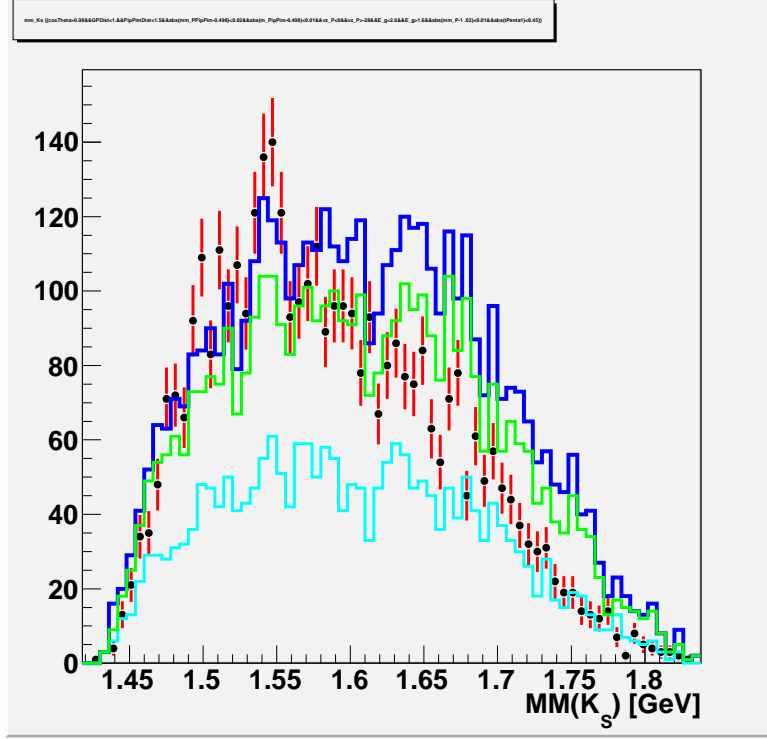
Figure 3: The distribution of MM(K_S) for g11 data with a cut $-t_\Theta < 0.45$ GeV^2 and g12 data with cuts: $-t_\Theta < 0.45$ GeV^2, $-t_\Theta < 0.55$ GeV^2 and $-t_\Theta < 0.6$ GeV^2 in order of increasing heights respectively. All histograms are for photon energy range $E_\gamma = 1.6 - 2.6$ GeV.

upper panel are the sum of data and MC histograms on the lower panel respectively.

In fig. 8 and fig. 9 similar distributions are presented for $t_\Theta < 0.5$ GeV^2 (left panels) and $t_\Theta < 0.55$ GeV^2 (right panels). As one can see general agreement of data and Monte Carlo simulated events is quite good, however systematically there is an excess of events at ≈ 1.54 GeV in all three set of plots with different upper limits on t_{Theta}, which is not described by the ϕ-MC.

In fig. 10 we present g11 and g12 data for photon energy range $E_\gamma = 1.75 - 2.1$ GeV with the $-t_\Theta < 0.45$ GeV^2 cut applied to g11 data and the
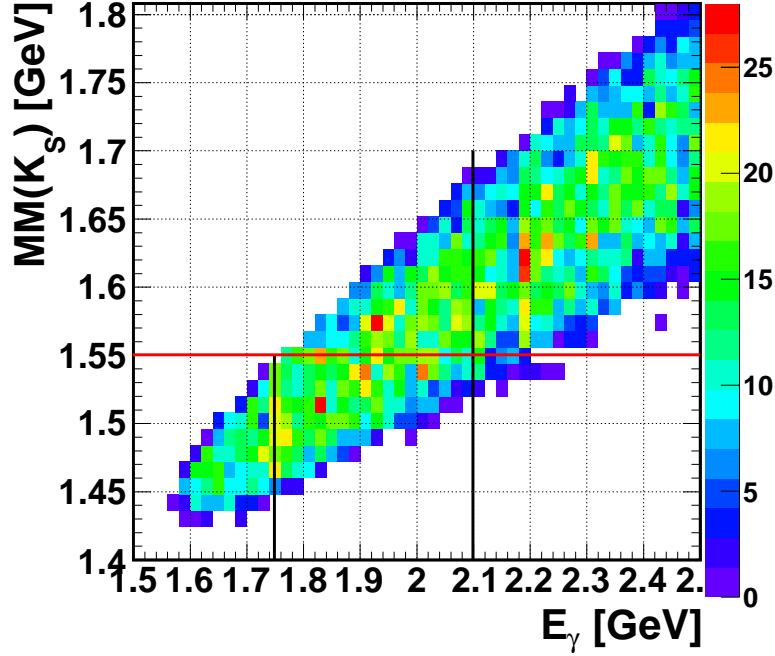
Figure 4: MM(K_S) versus E_γ.

$-t_\Theta < 0.6$ GeV^2 cut applied to g12 data. As one can see two histograms are very similar (left panel). On the right panel the sum of two data sets is presented with a fit using third order polynomial plus Gaussian function.

To see how compatible are two data sets: g11 and g12 we need to compare them in as close conditions as possible, it is not enough as we saw to take the same range of cuts. The spectra obtained from two data will be more consistent with each other if the range of photon energies are selected to be also such that variation of photon flux t_Θ are small compared to each other.

Such conditions are provided for the range of $E_\gamma = (1.75 - 2.1)$ GeV and $-t_\Theta < 0.45$ GeV^2. In fig. 11 (left panel) we present MM(K_S) from g11 and g12 data (g11 is normalized to total number of events with a
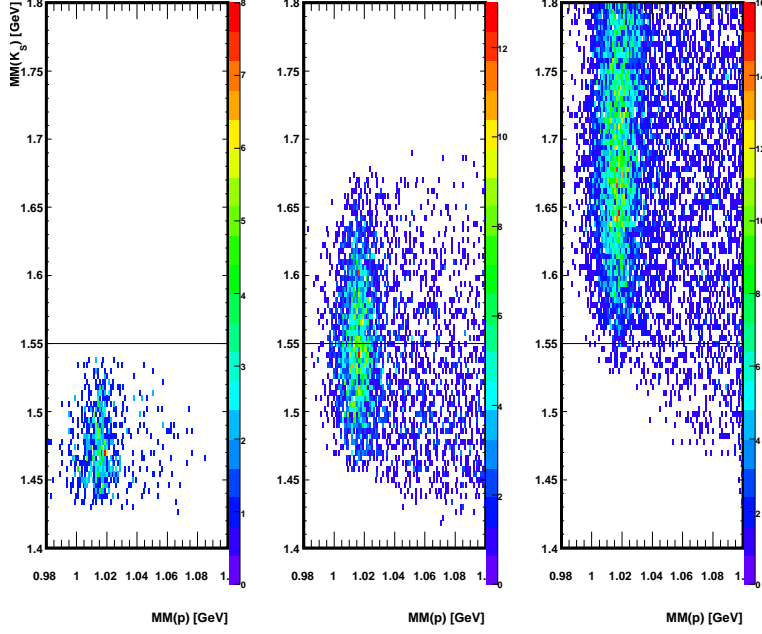
Figure 5: MM(K_S) versus MM(p) for three different photon energies: $E_\gamma < 1.75$ GeV (left panel), $E_\gamma = 1.75 - 2.1$ GeV (middle panel) and $E_\gamma > 2.1$ GeV (right panel).

factor 0.4). As one can see two histograms are compatible within statistical uncertainties, although g11 experiment has higher statistics. On the right panel is the sum of histograms from g11 and g12 data with a fit performed using polynomial plus Gaussian function.

In the following fig. 12 we plot the missing mass of kshort for the photon energy range $E_\gamma = (1.75 - 2.1)$ GeV and without any cut on t_Θ. As one can see statistically significant ($\approx 6\sigma$) resonanse structure is observed at ≈ 1.545 GeV.

To understand why it is possible to not apply the t-cut on g12 data at all, on next fig. 13 (lower left panel) we present the ratio of t_Θ distributions from g12 and g11 data for events selected under the ϕ peak and
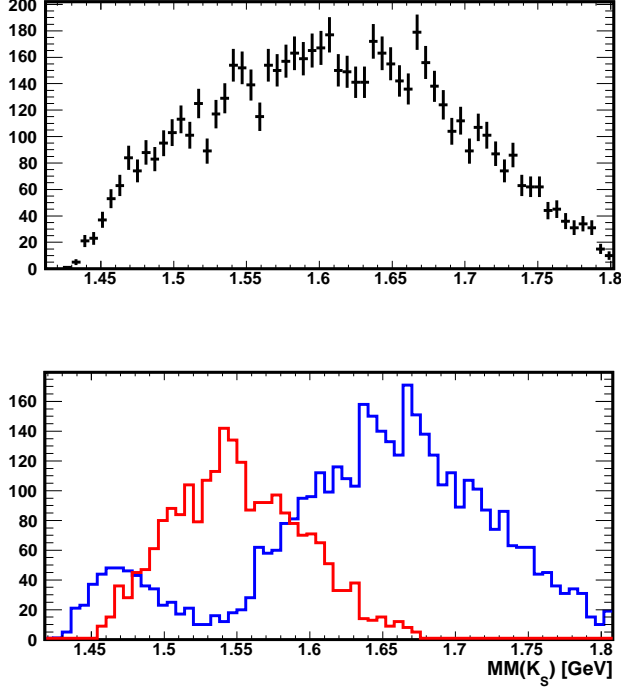
Figure 6: g12 data. Upper panel: $MM(K_S)$ with no cuts on t_Θ and $E_\gamma = 1.6 - 2.6$ GeV. Lower panel: red histogram is for the photon energy range $E_\gamma = 1.75 - 2.1$ GeV and the blue histogram for $E_\gamma < 1.75$ GeV and $E_\gamma > 2.1$ GeV combined again with no t_Θ cut.

in the range of $MM(K_S) = 1.54 \pm 0.03$ GeV. As one can see t-distribution drops exponentially faster in g12-, compared to g11 data. The reason for such a behavior is due to the shift of the hydrogen target position further upstream the beam line by 90 cm.

On the other hand the ratio of t_ϕ distributions from g12 and g11 in fig. 13 (right panel) in exactly the same conditions as of fig. 13 (left panel) shows that relative contribution at low t_ϕ is higher in g11 data compared to g12 data. This means that the landschaft of events distributed over two dimensions t_Θ and t_ϕ has a sharper increase with t_ϕ and slower rise in t_Θ for g11 versus g12 data. The corresponding 3-d
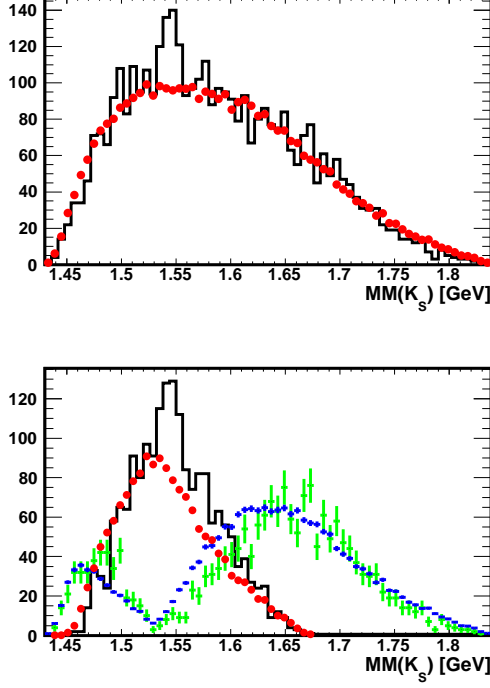
9

Figure 7: g11 data. Upper panel: $MM(K_S)$ for the photon energy range $E_\gamma = 1.6 - 2.6$ GeV with a cut $t_\Theta < 0.45$ GeV^2, red points are from ϕ-MC. Lower panel: black histogram is for the photon energy range $E_\gamma = 1.75 - 2.1$ GeV and green histogram is for $E_\gamma < 1.75$ GeV and $E_\gamma > 2.1$ GeV combined with $t_\Theta < 0.45$ GeV^2 cut for both histograms. Histograms with red and blue points are from ϕ-MC. Data and MC are normalized in the region of photon energies outside of the photon energy range $E_\gamma = 1.75 - 2.1$ GeV.

distributions are presented in fig. 13.

In conclusion we can state that already at this preliminary stage of g12 analysis it is clear that by limiting the range of photon energies to the relevant region of the overlap between ϕ meson and possible baryon resonance we reduce the difference between two measurements caused by very different acceptances.
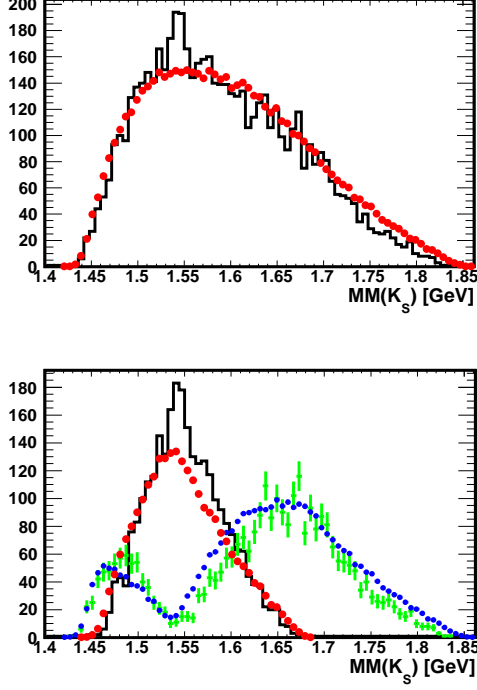
Figure 8: g11 data. Same as prefious figure for $t_\Theta < 0.5 \text{ GeV}^2$.

Moreover due to enhanced t_Θ acceptance the resonance structure in the missing mass of kshort manifiets itself withou the t_Θ-cut, which was the main obstacle in the recent review of ODU g11 analysis.

Although very many things are different in two experiments (except of essentially the shift crews) a good agreement is obtained between g11 and g12 data with a resonance structure observed at $\text{MM}(K_S) \approx 1.54$ GeV in both experiments. The g12 setup being originally tuned for another experiment, still provides statistically comparable data set and allows to make very important independent cross check of g11 experiment.
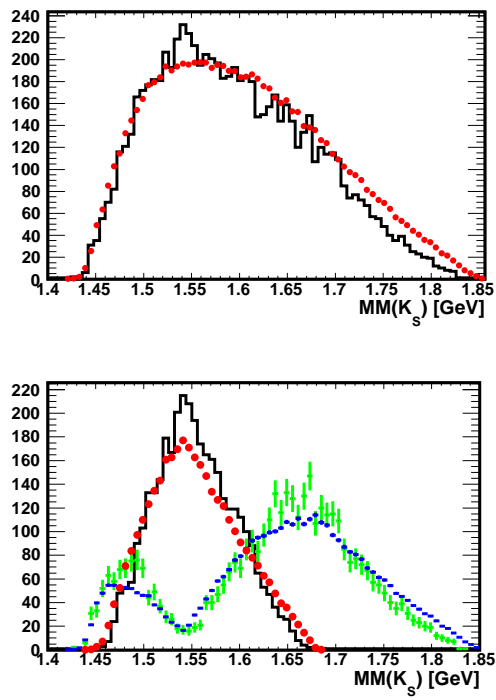
11

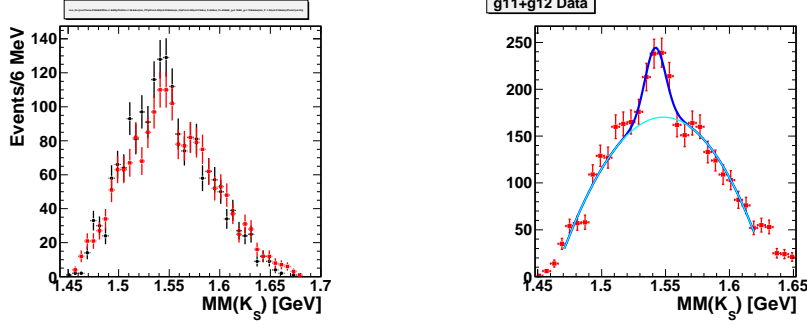Figure 9: g11 data. Same as previous figure for $t_\Theta < 0.55\,\mathrm{GeV}^2$.

Figure 10: Left panel: number of events versus MM(K_S) for g11 (black histogram) and g12 (red histogram). Right panel: the sum of g11 and g12 data. Both data sets have the same cuts $E_\gamma = (1.75 - 2.1)$ GeV; other cuts are $-t_\Theta < 0.45$ GeV^2 for g11- and $-t_\Theta < 0.6$ GeV^2 for g12 data.
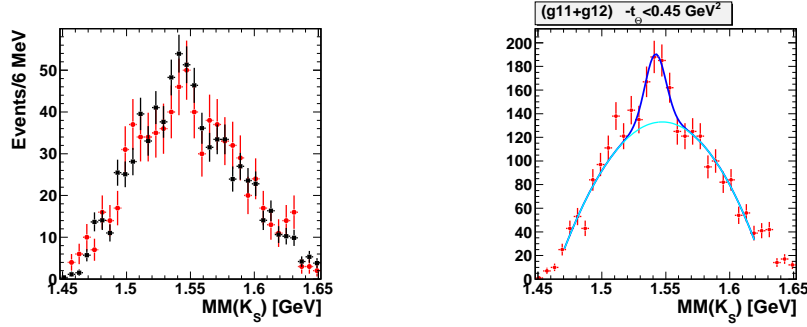

Figure 11: Left panel: number of events versus MM(K_S) for g11 (black histogram multiplied by 0.4) and g12 (red histogram). Right panel: the sum of g11 and g12 data. Both data sets have the same cuts $E_\gamma = (1.75 - 2.1)$ GeV and $-t_\Theta < 0.45$ GeV^2.

13

Figure 12: The missing mass $MM(K_S)$ from g12 data with no cut on t_Θ for the photon energy range $E_\gamma = (1.75 - 2.1)$ GeV.
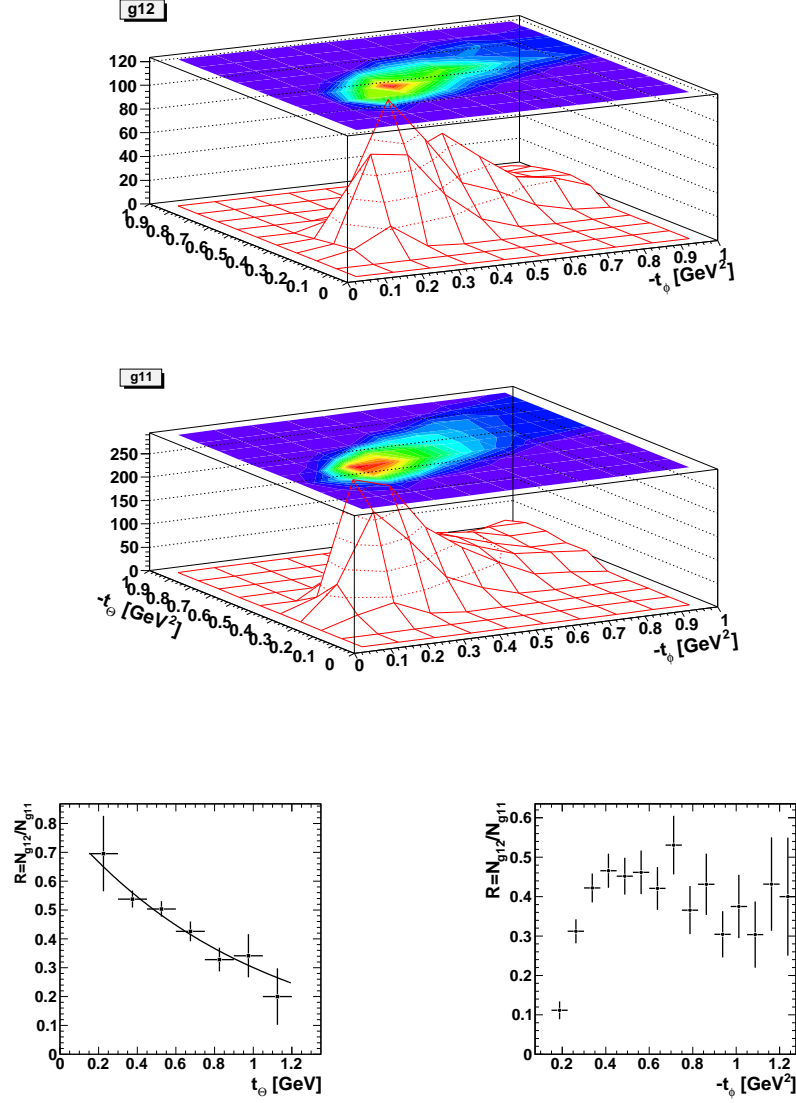
Figure 13: The 3-d distribution of events plotted versus t_ϕ and t_Θ for g12 and g11 data (upper panel). Events are selected under the ϕ peak $M_\phi \pm 0.02$ GeV and $\mathrm{MM}(K_S) = 1.54 \pm 0.03$ GeV for the photon energy range $E_\gamma = (1.75 - 2.1)$ GeV.Ratio of events from g12 to g11 data versus t_Θ (lower left panel) and versus t_ϕ (lower right panel).

15